Optics Communications 281 (2008) 4509–4514

Contents lists available at ScienceDirect

Optics Communications

journal homepage: www.elsevier.com/locate/optcom

Defect vector gap solitons in photonic lattices

Rui Wang [a,*], Cunxi Zhang [a], Lingmin Kong [a], Yongping Zhang [b]

[a] Department of Physics, ZheJiang Ocean University, ZhouShan 316000, China
[b] Institute of Physics, Chinese Academy of Sciences, Beijing 100190, China

ARTICLE INFO

Article history:
Received 22 March 2008
Received in revised form 7 May 2008
Accepted 7 May 2008

PACS:
42.65.Tg
42.65.Jx
42.65.Wi

ABSTRACT

The existence and general properties of different kinds of defect vector gap solitons in one dimensional optically induced photonic defect lattice with focusing saturable nonlinearity in photorefractive crystal are analyzed. The defect is well localized in a single site with two existence forms, namely repulsive and attractive defect. Propagation constants of two beams that compose defect vector gap solitons could be from same gap or from different gaps. We show that some kinds of unstable scalar defect gap solitons could be stabilized by their corresponding vector cases.

Broadening effect of pulse induced by diffraction or dispersion can be balanced by nonlinearity which results in solitons [1,2]. For light propagation in periodic media, the equilibrium between diffraction or dispersion with nonlinearity leads to gap solitons whose propagation constants lay in band gaps of corresponding linear system [3]. The study of gap solitons has attracted considerate attention. They have been investigated and observed in various kinds of system, such as waveguide arrays [4–7], optically induced photonic lattices [8,9] and in condensed matter physics due to the realization of Bose-Einstein condensations [10–12]. While gap solitons in two dimensional periodic structure have also been investigated extensively [13–15]. The propagation properties of gap solitons can be drastically changed if the light suffers from different nonlinear media. There are mainly three kinds of media which are intensively used to investigate the properties of gap solitons, they are kerr-type media, photorefractive media and nonlinear media with nonlocal effects [16]. The properties of gap solitons can be managed by changing periodic structure into superlattices [7,17].

If two beams that pass through the periodic system mutually self-trap in nonlinear media, they may form vector gap solitons if certain requirements are respected [1]. These self-localized states survive only when two components coexist, if one of them absent, these states are destroyed. The different kinds of vector gap solitons have been observed experimentally [18–21] and analyzed theoretically [22–25]. The stability of vector solitons in nonlocal nonlinear media has been investigated [26]. Even the surface vector gap solitons have been suggested [27].

On the other hand, the research about defect gap solitons has become an interesting field [28–31]. In Ref. [31], Yang and Chen have investigated the properties of defect gap solitons in an optically induced photonic lattices with focusing saturable nonlinearity in photorefractive crystal. The defect can be introduced in one period of periodic lattice through two forms, namely repulsive defect (the light intensity at defect site is lower than that at other sites) and attractive defect (light intensity at defect site is higher than that at other sites). The existence and general properties of defect gap solitons have been demonstrated in detail [31].

In this letter, we analyze the existence and stability properties of defect vector gap solitons in optically induced photonic lattices with a defect site and focusing saturable nonlinearity in photorefractive crystal. This system has been used to analysis defect gap solitons in Ref. [31] due to its experimentally accessible ability.

The setting contains optically induced defect photonic lattices and two mutually incoherent probe beams using two extraordinarily polarized beams. The propagation of probe beams can be described by coupled nonlinear Schrödinger equations under the slowly varying envelope approximation

$$\begin{aligned} i\frac{\partial \Psi_1}{\partial z}+\frac{\partial^2 \Psi_1}{\partial x^2}-\frac{E_0\Psi_1}{1+I_L(x)+|\Psi_1|^2+|\Psi_2|^2}=0 \\ i\frac{\partial \Psi_2}{\partial z}+\frac{\partial^2 \Psi_2}{\partial x^2}-\frac{E_0\Psi_2}{1+I_L(x)+|\Psi_1|^2+|\Psi_2|^2}=0 \end{aligned} \quad (1)$$

where Ψ_1 and Ψ_2 are the slowly varying envelopes of the probe beams, and they are coupled each other through cross-phase modulation. The probe beams propagate along z direction while periodic

* Corresponding author.
E-mail address: ruibaggio@sxu.edu.cn (R. Wang).

0030-4018/$ - see front matter © 2008 Elsevier B.V. All rights reserved.
doi:10.1016/j.optcom.2008.05.011

modulation of refractive index is in the transverse x direction. z is normalized to diffraction length $L_d = 2k_1D^2/\pi^2$, and x is in the unit of D/π. D is lattice spacing, $k_1 = k_0 n_e$ with $k_0 = 2\pi/\lambda_0$ is wave number, λ_0 is the wavelength in vacuum, n_e is unperturbed refractive index. E_0 labels the applied dc field and is normalized to $\pi^2/(k_0^2 n_e^4 D^2 r_{33})$ with r_{33} is the electro-optic coefficient of the crystal. I_L represents the intensity of photonic lattices with a single defect site at $x = 0$ [31]

$$I_L(x) = I_0 \cos^2(x)[1 + h e^{(-x^8/128)}] \tag{2}$$

I_0 is the peak intensity of lattices, normalized by $I_d + I_b$, here, I_d is the dark irradiance of the crystal corresponding to thermal generation of electrons in crystal kept in dark and I_b is the background illumination. h describes defect, when $h < 0$ the defect is repulsive one, while $h > 0$ the defect is attractive one. In experiment [32], the defect was introduced into uniform lattice by a specially designed amplitude mask. After passing through the mask, a spatially modulated partially coherent light beam became a periodic intensity pattern with a single defect. A small extraordinary component in the light beam maintained the defect during propagation of this pattern along photorefractive SBN (strontium barium niobate) crystal.

The Eq. (1) conserves powers $P_1 = \int_{-\infty}^{\infty} |\Psi_1|^2 \mathrm{d}x$, $P_2 = \int_{-\infty}^{\infty} |\Psi_2|^2 \mathrm{d}x$ and total power $P = P_1 + P_2$. The stationary solutions of the nonlinear coupled Schrödinger equations are

$$\Psi_{1,2}(z,x) = \Phi_{1,2}(x) \exp(-\mathrm{i}\mu_{1,2} z) \tag{3}$$

with $\mu_{1,2}$ are the propagation constants of each probe beams. $\Phi_{1,2}$ obey the following stationary coupled equations:

$$\begin{aligned} \frac{\partial^2 \Phi_1}{\partial x^2} - \frac{E_0 \Phi_1}{1 + I_L(x) + |\Phi_1|^2 + |\Phi_2|^2} + \mu_1 \Phi_1 = 0 \\ \frac{\partial^2 \Phi_2}{\partial x^2} - \frac{E_0 \Phi_2}{1 + I_L(x) + |\Phi_1|^2 + |\Phi_2|^2} + \mu_2 \Phi_2 = 0 \end{aligned} \tag{4}$$

In order to get defect vector gap solitons of Eq. (4), we must firstly know the band-gap structure of corresponding linear system without defect site. Then we will choose propagation constants of each beams in gaps of corresponding linear system and simulate Eq. (4) to get defect vector gap solitons numerically. The linear band-gap structure of Eq. (4) without defect site is shown in Fig. 1. Propagation constants of defect vector gap solitons lay in the gaps of corresponding linear system (blank areas in Fig. 1). The bottom blank area is semi-infinite gap which is called as the first gap, while the blank area nearest the first gap is called the second gap. The typical

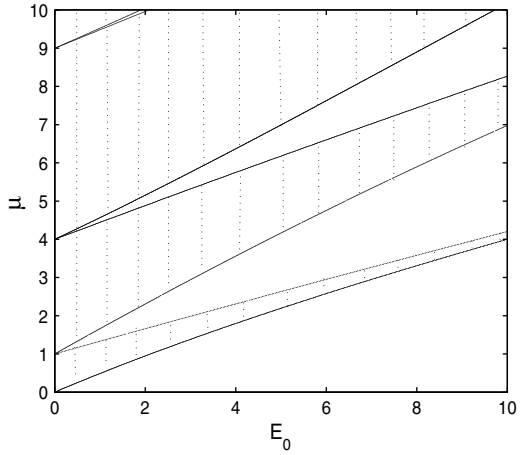

Fig. 1. Linear band-gap spectrum of corresponding linear system of Eq. (4) without defect site for $I_0 = 3$. Shadow areas are bands, while blank areas are gaps. The bottom blank area is semi-infinite gap called as the first gap. The blank area nearest the first gap is called as the second gap.

experiment parameters are given in Ref. [31], i.e. $D = 20$ μm, $\lambda_0 = 0.5$ μm, $n_e = 2.3$, and $\gamma_{33} = 280$ pm/V, then the unit of z corresponds to 2.3 mm, the unit of x corresponds to 6.4 μm, and the normalization of E_0 corresponds to 20 V/mm. We choose $I_0 = 3$ and $E_0 = 6$ through out the letter. In the following we derive defect vector gap solitons from same gap which means that propagation constants of probe beams lay in the same gap and from multigap which means that propagation constants of probe beams lay in different gaps. Eq. (4) are treated numerically with a standard relaxation method. After we deriving profiles of defect vector gap solitons, we perform linear stability analysis of those solutions by adding perturbation terms to the profiles

$$\begin{aligned} \Psi_{1,2}(z,x) = \{\Phi_{1,2}(x) + [v_{1,2}(x) - w_{1,2}(x)]\mathrm{e}^{\mathrm{i}\delta z} \\ + [v^*_{1,2}(x) + w^*_{1,2}(x)]\mathrm{e}^{-\mathrm{i}\delta z}\}\mathrm{e}^{-\mathrm{i}\mu_{1,2} z} \end{aligned} \tag{5}$$

where $\Phi_{1,2}$ are the profiles of defect vector gap solitons, $v_{1,2}(x)$ and $w_{1,2}(x)$ relate to perturbations. Substituting Eq. (5) into Eq. (1) and performing the standard linearization procedure around the stationary profiles $\Phi_{1,2}$, we derive the following linear eigenvalue problem:

$$\begin{pmatrix} 0 & \mathscr{L}_0 - \mu_1 & 0 & 0 \\ \mathscr{L}_1 & 0 & \mathscr{L}_2 & 0 \\ 0 & 0 & 0 & \mathscr{L}_0 - \mu_2 \\ \mathscr{L}_2 & 0 & \mathscr{L}_3 & 0 \end{pmatrix} \begin{pmatrix} v_1 \\ w_1 \\ v_2 \\ w_2 \end{pmatrix} = \delta \begin{pmatrix} v_1 \\ w_1 \\ v_2 \\ w_2 \end{pmatrix} \tag{6}$$

where

$$\begin{aligned} \mathscr{L}_0 &= -\frac{\partial^2}{\partial x^2} + \frac{E_0}{1 + I_L + \Phi_1^2 + \Phi_2^2} \\ \mathscr{L}_1 &= -\frac{\partial^2}{\partial x^2} - \mu_1 + \frac{E_0(1 + I_L - \Phi_1^2 + \Phi_2^2)}{(1 + I_L + \Phi_1^2 + \Phi_2^2)^2} \\ \mathscr{L}_2 &= -\frac{2\Phi_1 \Phi_2 E_0}{(1 + I_L + \Phi_1^2 + \Phi_2^2)^2} \\ \mathscr{L}_3 &= -\frac{\partial^2}{\partial x^2} - \mu_2 + \frac{E_0(1 + I_L + \Phi_1^2 - \Phi_2^2)}{(1 + I_L + \Phi_1^2 + \Phi_2^2)^2} \end{aligned} \tag{7}$$

here, δ are the eigenvalue. Once there exists an eigenvalue δ containing imaginary part, perturbations will grow exponentially as beams propagate along z direction, the corresponding stationary solutions $\Phi_{1,2}$ are unstable against perturbations. Otherwise, these stationary solutions are linear stable.

At first, we notice that when $\mu_1 = \mu_2$ there are kinds of defect vector gap solitons with the form $\Phi_1 = \Phi \sin\theta$ and $\Phi_2 = \Phi \cos\theta$, where θ is an arbitrary phase, and Φ just obey the scalar equation in Ref. [31], which have been carefully analyzed. Here, we are interested in the cases of $\mu_1 \neq \mu_2$. In the following, we concentrate on defect vector gap solitons with a twisted first component Φ_1 [24]. Fig. 2 shows defect gap solitons whose propagation constants lay in the first gap with attractive defect $h = 0.5$ and second component Φ_2 is the nodeless mode having a single peak located at the defect site (Fig. 2e). When fixing μ_1 there exist upper and lower cutoffs on μ_2. As shown in Fig. 2a, the existence domain of defect vector gap solitons enlarges with increasing μ_1, When μ_2 approaches lower cutoff, first twist component gradually vanishes and meanwhile second nodeless component becomes maximum, while as μ_2 approaches upper cutoff, second component gradually disappears for the empty circle case in Fig. 2a, and during the shrink, second nodeless component may evolve into a two obvious peaks structure in Fig. 2f and three peaks structure in Fig. 2h typically. However, for the solid circle case, the developed two humps structure from second component which locates around defect site symmetrically is not ceased to exist. Oppositely, there is a small regime near upper cutoff (the solid circles in Fig. 2a) where this two humps structure becomes enlarging and broadening with increas-

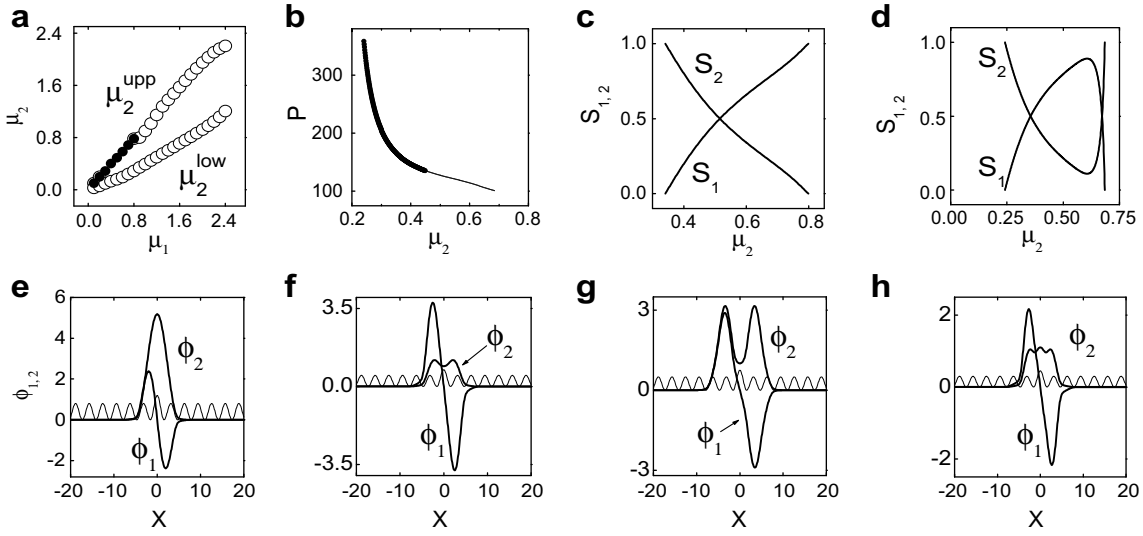

Fig. 2. Defect vector gap solitons with first twist and second nodeless modes from the first gap: (a) domain of existence of defect vector gap solitons at (μ_1, μ_2) plane, (b) the family of these vector gap solitons for $\mu_1 = 0.7$, thick line is stable while thin line is unstable, (c) and (d) dependence of energy sharing $S_{1,2} = P_{1,2}/P$ on μ_2 for $\mu_1 = 0.9$ and $\mu_1 = 0.7$, respectively, and (e)–(h) typical profiles of defect vector gap solitons at $(\mu_1, \mu_2) = (0.9, 0.4), (0.9, 0.74), (0.7, 0.675)$ and $(1.4, 1.2)$, respectively. Other parameters are $I_0 = 3$, $E_0 = 6$ and $h = 0.5$.

ing μ_2, at the same time, first component gradually vanishes. Fig. 2g shows this typical structure. This phenomenon is confirmed again by plots of the energy sharing of two components as the function of μ_2 for the empty circle case $\mu_1 = 0.9$ and the solid circle case $\mu_1 = 0.7$ in Fig. 2c and d, respectively. The energy sharing are defined as $S_{1,2} = P_{1,2}/P$. It is clearly shown that for the solid circle case (Fig. 2d) with decreasing μ_2 to lower cutoff, first component disappears, while with increasing μ_2 first component enlarges and second component shrinks at first, continuously increase μ_2 to a certain value, first component starts to shrink while second component which now develops into a two humps structure enlarges, when μ_2 reaches upper cutoff, the first component vanishes. Contrasting to Fig. 2d, for the empty circle case (Fig. 2c), second component shrinks to disappear at upper cutoff. The family of defect vector gap solitons shown in terms of the dependence of total power P on μ_2 at a fixed value of $\mu_1 = 0.7$ is demonstrated in Fig. 2b. The total power P decreases with increasing μ_2. Linear stability analysis shows that at the small μ_2 defect vector gap solitons are stable (the thick line in Fig. 2b), while increasing μ_2 to a threshold value, vector solitons become unstable (the thin line in Fig. 2b). Results of stability analysis are different from those of the nodeless modes in Fig. 6 of Ref. [31]. We conclude that the coexistence of twist and nodeless vector solitons could stabilize the nodeless modes which are unstable in the scalar case. In other words, unstable scalar gap solitons could be stabilized through cross-phase modulation in the vector case [24].

The propagation of defect vector gap solitons is performed by numerical simulating Eq. (1) with the initial profiles that are exact defect vector gap solitons in presence of random functions with Gaussian distribution and variance $\sigma_{1,2}^2 = 0.01$ in order to excite perturbations. Fig. 3a illustrates the propagation of defect vector gap soliton in Fig. 2e which are linear stable by linear stability analysis. The only second nodeless mode is shown and stable propagation confirms its stability. If we block first twist component, then propagate second component alone with perturbations, we find that second component is unstable in Fig. 3b. This verifies that the stable defect vector gap solitons will be destroyed in absence of one component. Defect vector gap solitons shown in Fig. 2f and h are unstable.

We also depict the existence region of μ_2 as a function of h for $\mu_1 = 0.9$ in Fig. 4. The profiles of defect vector gap solitons exist in

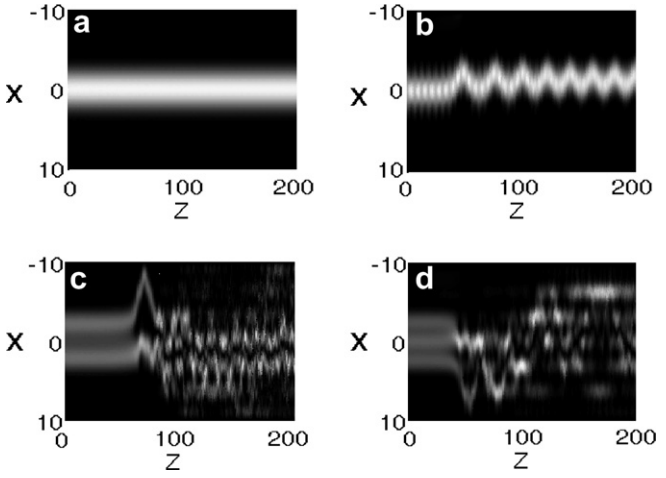

Fig. 3. Propagation of defect vector gap solitons shown in Fig. 2 in presence of Gaussian distributed random noise with variance $\sigma_{1,2}^2 = 0.01$. Only second component is shown: (a) corresponds to Fig. 2e, (b) second component of Fig. 2e as initial profile, while first component is blocked, (c) and (d) correspond to Fig. 2f and h, respectively.

this region are same as solitons discussed above. The dash line is a separator, in the left region of dash line, the behavior of vector gap solitons should be similar to that of solid circles case in Fig. 2a, i.e., as μ_2 approaches upper cutoff, second nodeless component evolves into a two humps structure and first twist component vanishes. While in the right side of dash line, when μ_2 approaches upper cutoff, second nodeless component ceases to exist. If μ_2 approaches lower cutoff, first component disappears no matter what sides of dash line. It is shown that lower cutoffs as well as upper cutoffs at the left side of dash line are nearly not changed as varying h, while the right area of dash line shrinks with increasing h. Defect vector gap solitons in the shadow areas are linear stable. The normal lattice case $h = 0$ belongs to left side of the dash line. Cutoff values of vector solitons for repulsive defect lattice $(h < 0)$ are almost same as those for normal lattice. Compared with the normal lattice case, the stability regions near lower cutoff for repulsive defect lattice are nearly not changed. While the stability regions near

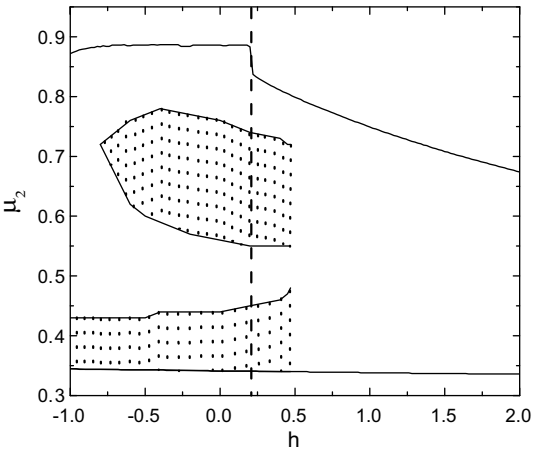

Fig. 4. The existence region of μ_2 as a function of h for a fixed value $\mu_1 = 0.9$. Defect vector gap solitons in the shadow areas are linear stable. Other parameter are $I_0 = 3$, $E_0 = 6$.

upper cutoff are raised and then shrink into a point with decreasing h. For attractive lattice case $h > 0$, the stability regions near lower cutoff are enlarged, while stability regions near upper cutoff are dropped with increasing h. However, when h is larger than 0.5, there are no any stable defect vector solitons.

We find defect vector gap solitons consisted of first triple-mode and second nodeless components [26]. The propagation constants of these solitons lay in the first gap. Typical profiles are shown in Fig. 5. The existence region of this kind of defect vector gap solitons in (h, μ_2) plane for a fixed $\mu_1 = 2$ shrinks with increasing h as demonstrated in Fig. 6a. For given μ_1 and h, as μ_2 approaches lower cutoff, first triple-mode component ceases to exist, while as μ_2 reaches upper cutoff, second nodeless component vanishes leaving only first component. Stability analysis result demonstrates the stable region of this kind of defect vector solitons is a small island shown in shadow area of Fig. 6a. The stability regions are enlarged for attractive defect lattice cases $(0 < h < 0.5)$ compared with that for normal lattice. Also the domain of existence of these solitons in (μ_1, μ_2) plane is depicted for $h = 0.5$ in Fig. 6b. Similar to Fig. 6a, at lower cutoff first triple-mode component disappears while at upper cutoff second nodeless component vanishes. The existence domain shrinks as decreasing μ_1. A typical family of these solitons is shown in Fig. 6c in terms of the dependence of total power P on μ_2 for $\mu_1 = 2$ and $h = 0.5$. The profiles of labeled points in Fig. 6c are demonstrated in Fig. 5. In Fig. 6d, the stability analysis result

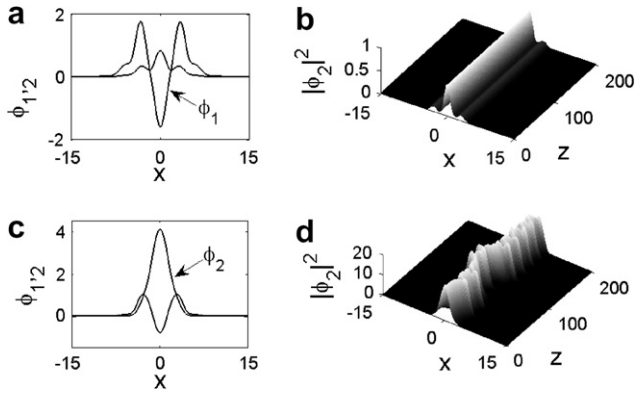

Fig. 5. Typical profiles of defect vector gap solitons composed by first triple-mode and second nodeless components corresponding to labeled points in Fig. 6c and their propagation: (a) and (b) $\mu_1 = 2$ and $\mu_2 = 1.75$, (c) and (d) $\mu_1 = 2$ and $\mu_2 = 0.7$. The perturbations are similar to these in Fig. 3 $h = 0.5$.

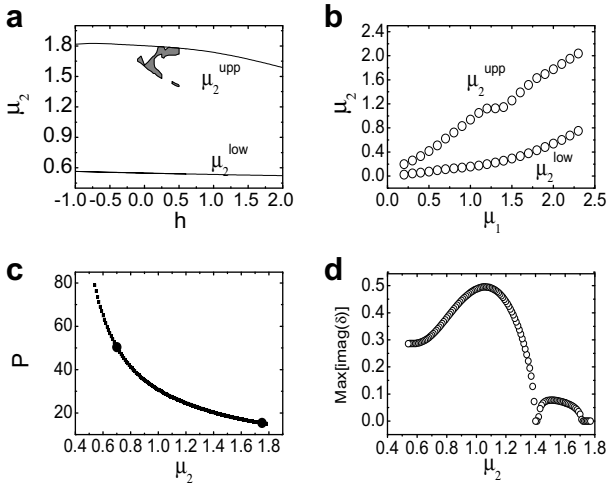

Fig. 6. Properties of defect vector gap solitons consisted of first triple-mode and second nodeless components from the first gap: (a) and (b) the existence domains in (h, μ_2) plane for $\mu_1 = 2$ and (μ_1, μ_2) plane for $h = 0.5$, respectively. Defect vector solitons in the shadow area of (a) belong to stable ones, (c) and (d) the typical family of these solitons and their corresponding linear stability analysis result with $\mu_1 = 2, h = 0.5$.

of the family reveals that unstable and stable regions alternate. This result is confirmed again by propagation of correspond solitons with perturbations in Fig. 5.

We have analyzed the existence and general properties of defect vector gap solitons whose propagation constants lay in the first gap. In the following, we demonstrate defect vector gap solitons from different gaps.

We first consider defect vector gap solitons composed by first twist component from the first gap and second component from the second gap. Though second component has a main peak located at the center of defect site symmetrically, it has an oscillatory tail structure which means it possesses an infinite number of nodes. This component is completely different from nodeless mode discussed above. The typical profiles are shown in Fig. 7c and f. The domain of existence of this kind of vector solitons in (μ_1, μ_2) plane (Fig. 7a) enlarges with increasing μ_1 for $h = -0.5$. Lower cutoff is not changed as varying μ_1, the value of lower cutoff corresponds to band edge $(\mu_2 = 2.9493)$. For $h = -0.5$ and a fixed value μ_1, as μ_2 approaches upper cutoff, second component vanishes, while as it reaches lower cutoff (band edge), second nodeless mode becomes highest and less localized with obvious quasiperiodic oscillatory tail structure. However, first twist component does not changed obviously, which means that the profile of first twist mode has no distinct change as varying μ_2 from lower cutoff to upper cutoff. We also show the existence region of this kind vector solitons in (h, μ_2) plane in Fig. 7b. It is clearly demonstrated that this kind of defect vector solitons only exist for repulsive defect case, and there are no the corresponding vector solitons in normal lattice and attractive defect lattice cases. The existence region shrinks quickly as increasing h and for $\mu_1 = 1.8$ it shrinks into a point at $h = -0.187$. The properties of vector solitons of Fig. 7b are resemblance to those in Fig. 7a, i.e., lower cutoff corresponds to band edge and when μ_2 reaches upper cutoff, second mode ceases to exist, while first twist component has no obvious change as varying of μ_2 from lower cutoff to upper cutoff. A family of these defect vector solitons and corresponding linear stability are depicted in Fig. 7d and e, respectively. The stability result of second component as scalar defect gap soliton reveals that the whole family is linear stable [31]. While, when it is bound with first twist component to form vector gap soliton, it becomes unstable in the middle of family as shown in Fig. 7e.

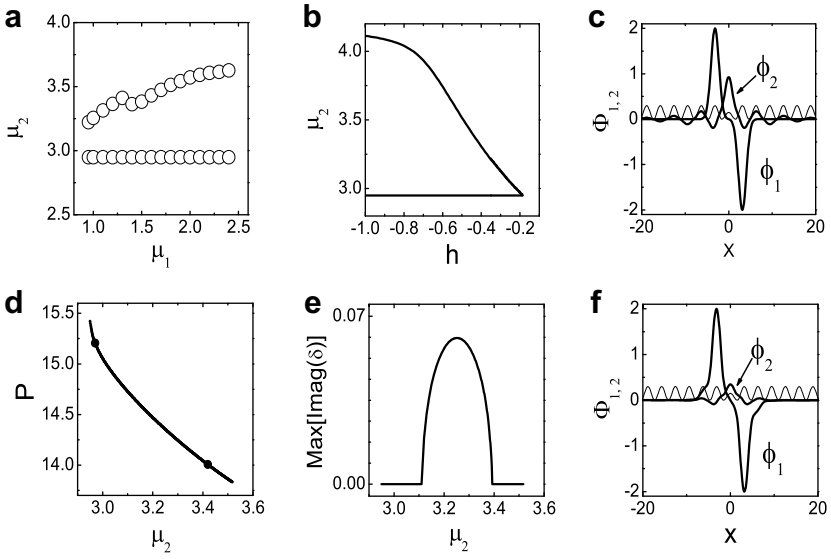

Fig. 7. Properties of defect vector gap solitons consisted of first twist mode from the first gap and second component with a main hump from the second gap: (a) and (b) existence domains of these vector solitons in (μ_1, μ_2) plane for $h = -0.5$ and (h, μ_2) plane for $\mu_1 = 1.8$, respectively, (d) and (e) family of these vector solitons and their corresponding linear stability analysis result, respectively with $\mu_1 = 1.8, h = -0.5$, (c) and (f) Profiles of these vector solitons corresponding to labeled points in (d) with $\mu_2 = 2.97$ for (c) and $\mu_2 = 3.42$ for (f).

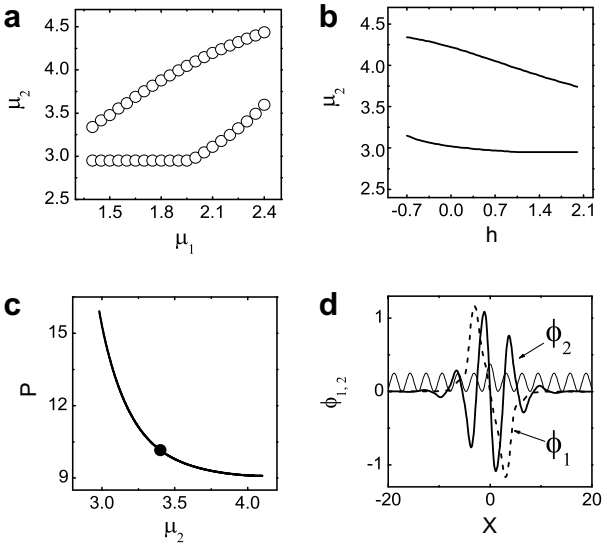

Fig. 8. Properties of defect vector gap solitons consisted of first twist component from the first gap and complex second component from the second gap: (a) and (b) existence domains of these vector solitons in (μ_1, μ_2) plane for $h = 0.5$ and (h, μ_2) plane for $\mu_1 = 2$, respectively, (c) family of these vector solitons with $\mu_1 = 2, h = -0.5$, and (d) profile of vector solitons corresponding to labeled point in (c) with $\mu_2 = 3.4$.

Another kinds of defect vector gap solitons are shown in Fig. 8. These vector solitons consist of first twist component from the first gap and complex second component from the second gap (in Fig. 8d). The complex second component has been analyzed as scalar defect mode in Fig. 9 of Ref. [31]. We show the existence domain of this kind of vector solitons in Fig. 8a with $h = 0.5$ in (μ_1, μ_2) plane. It is clearly demonstrated that there is a critical value of μ_1, when μ_1 is smaller than the critical value, lower cutoff of μ_2 is just band edge, while μ_2 larger than the critical value, lower cutoff of μ_2 increases with increasing of μ_1. As μ_2 approaches upper cutoff, complex second component vanishes leaving only first component. If μ_1 is larger than the critical value, as μ_2 approaches lower cutoff, first twist component ceases to exist. While if μ_1 is smaller than the critical value, as μ_2 reaches lower cutoff (band edge), first component is still present. The domain existence area of these vector solitons in (h, μ_2) with $\mu_1 = 2$ is shown in Fig. 8b. The area shrinks as increasing h. Compared with the normal lattice case $h = 0$, the existence regions for repulsive defect lattice cases are enlarged with decreasing h, while the existence regions for attractive lattice are reduced with increasing h. When μ_2 reaches upper cutoff first twist component vanishes and as μ_2 accesses lower cutoff second component disappears. Fig. 8c presents a family of this kind of vector solitons. Linear stability analysis shows that the whole family in Fig. 8c are unstable. However, as scalar gap solitons , some second components are stable in Ref. [31].

In conclusion, we have demonstrated the existence and general properties of different kinds of defect vector gap solitons in one dimensional optically induced photonic lattice with a well localized defect site in photorefractive crystal. We consider the focusing saturable nonlinearity case. There are two ways that the defect exists, namely, repulsive and attractive defect [31]. Two beams are bound together incoherently to form the vector gap solitons. Propagation constants of these two beams could be from same gap (the first gap as an example) and from different gaps (the first and second gaps) [22,23]. The behaviors of defect vector gap solitons might be completely different from their scalar corresponding case. We show that some unstable scalar defect gap solitons could be stabilized by binding them with other kinds of gap solitons to form vector gap solitons. This would make the observation of these unstable scalar defect gap solitons becoming possible in experiment. While some stable scalar defect gap solitons could be unstable in their corresponding vector cases.

References

[1] G.I. Stegeman, M. Segev, Science 286 (1999) 1518.
[2] D.N. Christodoulides, F. Lederer, Y. Silberberg, Nature 424 (2003) 817.
[3] P. Meystre, Atom Optics, Springer-Verlag, New York, 2001.
[4] Jason W. Fleischer, Tal Carmon, Mordechai Segev, Nikos K. Efremidis, Demetrios N. Christodoulides, Phys. Rev. Lett. 90 (2003) 023902.
[5] D. Mandelik, R. Morandotti, J. Aitchison, Y. Silberberg, Phys. Rev. Lett. 92 (2004) 093904.
[6] E. Smirnov, C.E. Rüter, D. Kip, Y.V. Kartashov, L. Torner, Opt. Lett. 32 (2007) 1950.
[7] Andrey A. Sukhorukov, Yuri S. Kivshar, Opt. Lett. 28 (2003) 2345.
[8] D. Neshev, E. Ostrovskaya, Y. Kivshar, W. Krolikowski, Opt. Lett. 28 (2003) 710.

[9] D. Neshev, Andrey A. Sukhorukov, B. Hanna, W. Krolikowski, Yuri S. Kivshar, Phys. Rev. Lett. 93 (2004) 083905;
B. Hanna, W. Krolikowski, D. Neshev, A.A. Sukhorukov, E.A. Ostrovskaya, Yuri S. Kivshar, Opto-Electron. Rev. 13 (2005) 85.
[10] B. Eiermann, Th. Anker, M. Taglieber, P. Treutlein, K.-P. Marzlin, M.K. Oberthaler, Phys. Rev. Lett. 92 (2003) 230401.
[11] P.J. Louis, E.A. Ostrovskaya, C.M. Savage, Yuri S. Kivshar, Phys. Rev. A 67 (2003) 013602.
[12] N.K. Efremidis, D.N. Christodoulides, Phys. Rev. A 67 (2003) 063608.
[13] Z. Chen, H. Martin, E.D. Eugenieva, J. Xu, A. Bezryadina, Phys. Rev. Lett. 92 (2004) 143902.
[14] C. Lou, X. Wang, J. Xu, Z. Chen, J. Yang, Phys. Rev. Lett. 98 (2007) 213903.
[15] E.A. Ostrovskaya, Yuri S. Kivshar, Phys. Rev. Lett. 90 (2003) 160407.
[16] Z. Xu, Y.V. Kartashov, L. Torner, Phys. Rev. Lett. 95 (2005) 113901.
[17] P.J. Louis, E.A. Ostrovskaya, Yuri S. Kivshar, Phys. Rev. A 71 (2005) 023612.
[18] Z. Chen, M. Acks, E.A. Ostrovskaya, Yuri S. Kivshar, Opt. Lett. 25 (2000) 417.
[19] J. Meier, D.N. Christodoulides, G. Stegeman, Y. Silberberg, R. Morandotti, J.S. Aitchison, Phys. Rev. Lett. 91 (2003) 143907.
[20] Z. Chen, A. Bezryadina, I. Makasyuk, J. Yang, Opt. Lett. 29 (2004) 1656.
[21] R.A. Vencencio, E. Smirnov, C.E. Rüter, D. Kip, M. Stepia, Phys. Rev. A 76 (2007) 033816.
[22] O. Cohen, T. Schwartz, J.W. Fleischer, M. Segev, D.N. Christodoulides, Phys. Rev. Lett. 91 (2003) 113901.
[23] A.A. Sukhorukov, Y.S. Kivshar, Phys. Rev. Lett. 91 (2003) 113902.
[24] Y.V. Kartashov, A.S. Zelenina, V.A. Vysloukh, L. Torner, Phys. Rev. E 70 (2004) 066623.
[25] E.P. Fitrakis, P.G. Kevrekidis, B.A. Malomed, D.J. Frantzeskakis, Phys. Rev. E 74 (2006) 026605.
[26] Z. Xu, Y.V. Kartashov, L. Torner, Phys. Rev. E 73 (2006) 055601(R).
[27] Y.V. Kartashov, F. Ye, L. Torner, Opt. Express 14 (2006) 4808;
Y.V. Kartashov, L. Torner, V.A. Vysloukh, Opt. Lett. 31 (2006) 2595.
[28] P.G. Kevrekidis, Y.S. Kivshar, A.S. Kovalev, Phys. Rev. E 67 (2003) 046604.
[29] F. Fedele, J. Yang, Z. Chen, Opt. Lett. 30 (2005) 1506.
[30] F. Fedele, J. Yang, Z. Chen, Stud. Appl. Math. 115 (2005) 279.
[31] J. Yang, Z. Chen, Phys. Rev. E 73 (2006) 026609.
[32] Igor Makasyuk, ZhigangChen, Jianke Yang, Phys. Rev. Lett. 96 (2006) 223903.